A comparative analysis of frog early development

Eugenia M. del Pino*†, Michael Venegas-Ferrín*, Andrés Romero-Carvajal*, Paola Montenegro-Larrea*, Natalia Sáenz-Ponce*, Iván M. Moya*, Ingrid Alarcón*, Norihiro Sudou‡, Shinji Yamamoto‡, and Masanori Taira‡

*Escuela de Ciencias Biológicas, Pontificia Universidad Católica del Ecuador, Avenida 12 de Octubre 1076 y Roca, Quito, Ecuador; and ‡Department of Biological Sciences, Graduate School of Science, University of Tokyo, Hongo 7-3-1, Bunkyo-ku, Tokyo 113-0033, Japan

This contribution is part of the special series of Inaugural Articles by members of the National Academy of Sciences elected on April 25, 2006.

Contributed by Eugenia M. del Pino, May 31, 2007 (sent for review April 24, 2007)

The current understanding of *Xenopus laevis* development provides a comparative background for the analysis of frog developmental modes. Our analysis of development in various frogs reveals that the mode of gastrulation is associated with developmental rate and is unrelated to egg size. In the gastrula of the rapidly developing embryos of the foam-nesting frogs *Engystomops coloradorum* and *Engystomops randi*, archenteron and notochord elongation overlapped with involution at the blastopore lip, as in *X. laevis* embryos. In embryos of dendrobatid frogs and in the frog without tadpoles *Eleutherodactylus coqui*, which develop somewhat more slowly than *X. laevis*, involution and archenteron elongation concomitantly occurred during gastrulation; whereas elongation of the notochord and, therefore, dorsal convergence and extension, occurred in the postgastrula. In contrast, in the slow developing embryos of the marsupial frog *Gastrotheca riobambae*, only involution occurred during gastrulation. The processes of archenteron and notochord elongation and convergence and extension were postgastrulation events. We produced an Ab against the homeodomain protein Lim1 from *X. laevis* as a tool for the comparative analysis of development. By the expression of Lim1, we were able to identify the dorsal side of the *G. riobambae* early gastrula, which otherwise was difficult to detect. Moreover, the Lim1 expression in the dorsal lip of the blastopore and notochord differed among the studied frogs, indicating variation in the timing of developmental events. The variation encountered gives evidence of the modular character of frog gastrulation.

Brachyury | *Gastrotheca* | Lim1

The current understanding of the molecular mechanisms of early development in *Xenopus laevis* (1) provides the basis for comparative studies with other frogs. In fact, it is well known that the morphology of the gastrula and the timing of developmental events differ greatly among frogs, although the molecular mechanisms underlying development of frogs other than *X. laevis* are unknown. Although it is possible that the early gene expression patterns in embryos of different frogs may follow the *X. laevis* pattern, we hypothesize that the timing of gene expression differs according to the rate of development. In *X. laevis*, which has a fast developmental rate, gene expression at the dorsal lip of the blastopore is extraordinarily complex (reviewed in ref. 1) because of the overlap of developmental processes. In frogs that develop more slowly than *X. laevis*, it may be possible to observe a separation of these gene expression domains. As a molecular tool to address this issue, we developed an antibody against the *X. laevis* homeodomain protein Lim1 and compared Lim1 expression in the dorsal lip of the blastopore of *X. laevis* with other frog embryos. Moreover, we compared the morphology of the circumblastoporal collar (CBC) and the elongation of the archenteron and notochord during gastrulation in embryos of frogs with different reproductive strategies, egg size, and developmental time to document the characteristics of gastrulation patterns. For this comparative analysis, we chose the marsupial frog *Gastrotheca riobambae*, several species of dendrobatid frogs (genus *Colostethus*, *Epipedobates*, and *Dendrobates*), two foam-nesting frogs (genus *Engystomops*), and a frog without tadpoles (*Eleutherodactylus coqui*).

Embryos of the marsupial frog *G. riobambae* develop slowly inside a dorsal pouch of the mother, and large tadpoles are released after an average of 120 days of incubation (2). This reproductive mode is characterized by large eggs and slow development. The time required from fertilization to the end of gastrulation is 14 days for *G. riobambae*, whereas, in *X. laevis*, the embryos it is only 14 h (3, 4).

During gastrulation, the embryos of *G. riobambae* form an embryonic disk from which the body of the embryo is derived. This pattern resembles development of the chick, although the *G. riobambae* embryos have holoblastic cleavage and form a blastopore with involution at the lip of the blastopore (5, 6). At the onset of gastrulation [stage (st) 10], the blastoporal rim develops around the future yolk plug (7). This feature has not been described for other frogs. At the vegetal pole, cells undergo vegetal contraction as in *X. laevis* and other frogs (6, 8, 9). Thereafter, bottle cells occur on the dorsal side, before the formation of the faint dorsal lip of the blastopore (7). In contrast, the delimitation of the blastopore is gradual in embryos of *X. laevis* and of the dendrobatid frog, *Colostethus machalilla* (7, 10).

In *G. riobambae* embryos, elongation of the archenteron and notochord and dorsal convergence and extension (CE) occur after closure of the blastopore (4), in marked contrast to *X. laevis*. The cells that involuted during gastrulation remain in the blastopore lip, which consequently thickens to form a large CBC and embryonic disk (7). In *X. laevis*, in contrast, CE movements begin in the midgastrula. The early occurrence of CE is associated with movement of the involuted cells away from the lip of the blastopore and with elongation of the archenteron and notochord. The cell movements of CE and convergence and thickening are important forces in the closure of the *X. laevis* blastopore (11, 12).

The question we would like to address is whether the subtle dorsal lip of the blastopore of *G. riobambae* embryos is equivalent to the *X. laevis* organizer. As a first approach, we analyzed the expression of the homeodomain protein Lim1 in the dorsal lip of the blastopore of *G. riobambae* embryos in comparison with other frogs. The homeodomain gene *Xlim1* is one of the first described genes with organizer activity (13). Thereafter, the *X. laevis* organizer has been characterized by the expression of numerous genes, reviewed in ref. 1. In embryos of *X. laevis* and other vertebrates, *Xlim1* plays a role in mesoderm induction,

Author contributions: E.M.d.P. designed research; E.M.d.P., M.V.-F., A.R.-C., P.M.-L., N.S.-P., I.M.M., I.A., N.S., S.Y., and M.T. performed research; N.S., S.Y., and M.T. contributed new reagents/analytic tools; E.M.d.P., M.V.-F., A.R.-C., P.M.-L., and N.S.-P. analyzed data; and E.M.d.P. wrote the paper.

The authors declare no conflict of interest.

Abbreviations: Bra, Brachyury; CBC, circumblastoporal collar; CE, dorsal convergence and extension; cnc, cranial neural crest; NCAM, neural cell adhesion molecule; st (*n*), stage.

†To whom correspondence should be addressed at: Pontificia Universidad Católica del Ecuador, Escuela de Ciencias Biológicas, Apartado 17–01-2184, Avenida 12 de Octubre 1076 y Roca, Quito, Ecuador. E-mail: edelpino@puce.edu.ec.

mesoderm and neural development, the development of anterior structures of the head, and in the movements of gastrulation (13–18). By the expression of Lim1, we identified the dorsal lip of the blastopore, the notochord and, consequently, the onset of CE, the pronephros, and neural cells in the embryos of various frogs.

In embryos of the dedrobatid frogs, *C. machalilla* and *Epipedobates anthonyi*, the lip of the blastopore and the CBC thicken during gastrulation because of the accumulation of involuted cells. Moreover, CE occurs after blastopore closure, as in *G. riobambae* but without formation of an embryonic disk. In contrast, elongation of the archenteron begins in the midgastrula (7, 19, 20). It is of interest to know whether the gastrulation pattern is altered in dendrobatid frogs with much larger eggs. The eggs of *C. machalilla*, at 1.6 mm in diameter, are the smallest yet observed among dendrobatids. In *E. anthonyi* and *Epipedobates tricolor*, egg diameter approaches 2 mm, and in *Epipedobates ingeri*, the egg measures 3 mm in diameter, which is the size of the *G. riobambae* egg. Even larger eggs, of 3.5 mm in diameter, were found in *Dendrobates auratus.* Eggs of this diameter are equivalent in size to the eggs of *E. coqui*, the frog without tadpoles. Embryos of dendrobatid frogs are incubated in terrestrial nests for 19–21 days, when tadpoles emerge, and the embryos take 4–6 days from fertilization to the end of gastrulation. Development is somewhat slower in *E. ingeri* and *D. auratus*, dendrobatid frogs with larger eggs. Therefore, cleavage and gastrulation in dendrobatids have an intermediate rate between the fast development of *X. laevis* and the slow development of *G. riobambae*. In addition, we analyzed the gastrulation mode of the foam-nesting frogs *Engystomops coloradorum* and *Engystomops randi* (Leptodactylidae), and we provide a description of their early development. Their eggs measure 1.3 and 1.1 mm in diameter, respectively, and require 24 h from the time of fertilization to the end of gastrulation, a rate of development that approaches *X. laevis*. Foam-nesting frogs are appropriate for developmental studies because they breed in captivity, have synchronous oogenesis (21, 22), as previously demonstrated for *Engystomops pustulosus*, and their embryos can be easily manipulated.

The rate of early development of the frog with direct development, *E. coqui* (Leptodactylidae), is only slightly slower than that of *X. laevis*, although its eggs are large (3.5 mm in diameter) (23). The terrestrial embryos of *E. coqui* not only lack tadpoles but also have precocious development of the limbs (24). Our analysis of Lim1 expression in the *G. riobambae* gastrula and the comparison of development among frogs with different developmental rates and egg sizes contribute to further characterize frog developmental patterns.

Results

Development of *E. coloradorum*. We studied the morphology of *E. coloradorum* embryos from fertilization to hatching. During amplexus in *E. coloradorum*, the eggs became enclosed in a foam nest that derived from the egg jelly and floated in the water (Fig. 1*A*). Within the foam nest, embryonic development synchronously advanced until the tadpole stage (Fig. 1 *B–J*). At hatching, the tadpoles moved into the underlying water. Development to hatching required 4 days in *E. coloradorum* in comparison with 2 days in *X. laevis*. The foam nest contained from 100 to 120 small eggs of white appearance, and, because of their light color, the eggs were camouflaged in the white foam of the nest (Fig. 1 *A* and *B*). The jelly foam was manually removed, and the white embryos resembled albino *X. laevis* embryos (Fig. 1*B*). At later stages, however, the embryos developed pigment around nuclei (data not shown), which was bleached for the observation of immunostaining patterns.

The external appearance of cleavage and gastrula embryos of *E. coloradorum* resembled the embryos of *X. laevis* (Fig. 1 *C–E*) and were staged according to the *X. laevis* table of stages (3). The neurula and tailbud embryos, however, differed significantly (Fig. 1 *F–H*), and after st 14, the embryos were staged according to Gosner (25). The body of the *E. coloradorum* tailbud embryo was curved around the yolk (Fig. 1 *G* and *H*). As development advanced, the embryos became elongated and developed external gills and the heart (Fig. 1*I*). At hatching, the external gills were extended, and the embryos were slightly pigmented (Fig. 1*J*). The developmental pattern of *E. randi* was similar to that of *E. coloradorum* (data not shown).

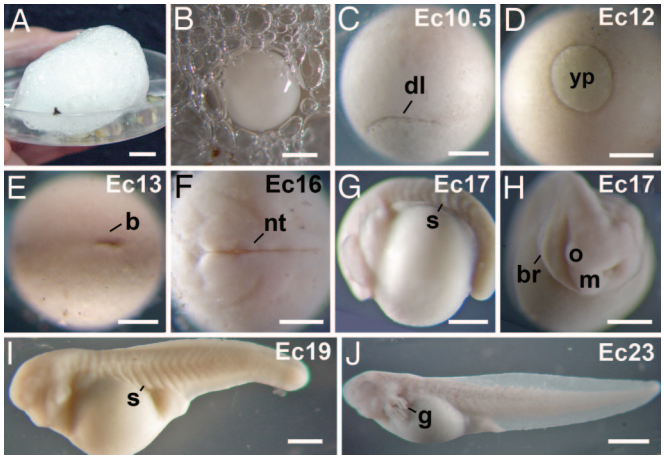

Fig. 1. Development from fertilization to hatching of the foam nesting frog *E. coloradorum.* (*A*) Foam nest. (*B*) Egg within the jelly foam. (*C*) Dorsal lip stage (12 h). In this and the following stages, the time after fertilization is given in hours. (*D*) Midgastrula (18 h). (*E*) Postgastrula (23 h). (*F*) Neurula (29 h). (*G*) Tailbud (34 h). (*H*) Head region of the embryo shown in *G*. (*I*) Development of the gills and the heart (51 h). (*J*) Tadpole at hatching (96 h). In this and the following figures, the numbers in the upper right hand corner gives the developmental stage, and the letters indicate the species: Cm, *C. machalilla*; Da, *D. auratus*; E, *E. coqui*; Ec, *E. coloradorum*; Ea, *E. anthonyi*; Ei, *E. ingeri*; Er, *E. randi*; Et, *E. tricolor*; Gr, *G. riobambae*; X, *X. laevis*; b, blastopore; br, branchial arches; dl, dorsal lip; g, gills; m, mandibular arch; nt, neural tube; o, optic vesicle; s, somite; yp, yolk plug. [Scale bars: 400 μm (*C–H*); 500 μm (*I*); 550 μm (*B*); 1,000 μm (*J*); and 1 cm (*A*).]

Gastrulation Patterns. The features of gastrulation in the marsupial frog *G. riobambae* and the dendrobatid frog *E. anthonyi* are given to allow comparison, although these patterns were already reported (5, 7). An embryonic disk that contained small cells, derived from the blastopore lip, developed during *G. riobambae* gastrulation (Fig. 2 *A* and *B*). Underneath, the archenteron was very small (Fig. 2*B*). In contrast, an embryonic disk was not found in the gastrula of the dendrobatid frogs *C. machalilla* and *E. anthonyi* (7). The involuted cells, however, accumulated in the blastopore lip and formed a large CBC (Fig. 2*C*). Elongation of the archenteron started in the midgastrula of these dendrobatid frogs (7).

The gastrulae of dendrobatids varied greatly in size (Fig. 2*D*). Nevertheless, a comparable CBC was formed in the embryos of *E. anthonyi*, *E. tricolor*, *E. ingeri*, and *D. auratus* (Fig. 2 *C* and *E–G*), although its size was smaller in *D. auratus* despite the fact that its eggs are among the biggest studied. In addition, elongation of the archenteron began earlier in dendrobatid embryos with big eggs (data not shown). The onset of CE is unknown in the large dendrobatid embryos of *E. tricolor*, *E. ingeri*, and *D. auratus*.

In contrast, in the foam-nesting frog *E. coloradorum*, the archenteron and notochord started their elongation in the midgastrula, and thus, gastrulation in this frog resembled the pattern in *X. laevis* (Fig. 2 *H* and *I*). Notochord elongation was detected

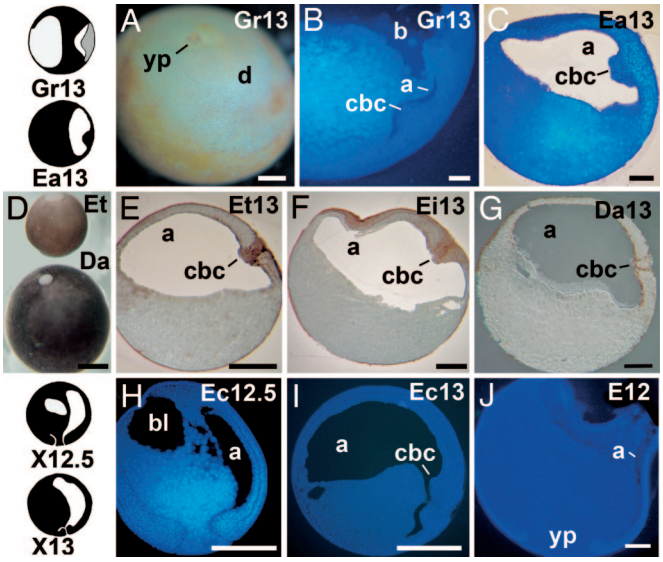

Fig. 2. The CBC in frog eggs of different size. (*A* and *B*) Embryos of *G. riobambae* (3 mm in diameter). (*A*) The embryonic disk in an embryo stained for the cell borders. (*B*) Sagittal section from a st-13 gastrula stained for cell nuclei. The CBC is thick, and the archenteron is small. (*C*) Late gastrula of *E. anthonyi* (2 mm in diameter) stained for cell nuclei. (*D*) Size comparison between *E. tricolor* and *D. auratus* gastrulae. (*E*) Gastrula of *E. tricolor* (2 mm in diameter). (*F*) Gastrula of *E. ingeri* (3 mm in diameter). (*G*) Gastrula of *D. auratus* (egg, 3.5 mm in diameter). (*H*) Midgastrula of *E. coloradorum* (1.3 mm in diameter). (*I*) Late gastrula of *E. coloradorum*. (*J*) Midgastrula of *E. coqui* (3.5 mm in diameter). The drawings on the left give the outlines in sagittal view of *G. riobambae*, *E. anthonyi*, and *X. laevis* embryos. The embryonic disk, which includes the CBC, is shown in gray. a, archenteron; bl, blastocoel; cbc, circumblastoporal collar; d, disk; yp, yolk plug. [Scale bars: 250 μm (*B*, *C*, and *G*); 500 μm (*A*, *E*, *F*, and *H–J*); and 1 mm (*D*).]

by the expression of Lim1 (data not shown). Likewise, the archenteron elongated during gastrulation in the large and rapidly developing embryos of *E. coqui*, the frog without tadpoles. Moreover, the blastopore lip was thin, because the involuted cells moved away from the blastopore lip (Fig. 2*J*). These features resembled the *X. laevis* gastrulation mode. In contrast with *X. laevis*, the movements of CE were retarded until after blastopore closure, as evidenced by the expression of *Ecbra* in the notochord (26). This difference indicates that the extensive elongation of the *E. coqui* archenteron that occurs during gastrulation is guided by forces other than CE.

Lim1 Expression in the Gastrula of *X. laevis* and *G. riobambae*. A recently prepared Ab against *X. laevis* Lim1 appears to be more effective for staining of early embryos than a previously described Ab (27), reacting strongly with deep nuclei of the dorsal blastopore lip of st-10.5 embryos of *X. laevis* (Fig. 3*A*). Additionally, a few Lim1-positive nuclei were detected in surface cells of the dorsal lip of the blastopore (data not shown). Moreover, Lim1-positive nuclei were found in deep cells of the lateral and ventral regions, delimiting a ring around the future yolk plug. There was a clear distinction between dorsal and ventral sides, because Lim1-positive nuclei were more abundant in the dorsal side. In st-13 embryos, Lim1 expression was detected in deep cells of the anterior region of the archenteron roof and in the notochord (Fig. 3*B*). In embryos of st 22, the presumptive pronephros (Fig. 3*C*) and specific cells of the CNS (Fig. 3*D*) were Lim1-positive. These results are in agreement with the previously described expression of the gene *Xlim1* in *X. laevis* embryos (15, 16, 27). Moreover, the expression of Lim1 in embryos of other frogs could be analyzed because anti-Lim1 cross-reacted with other frogs.

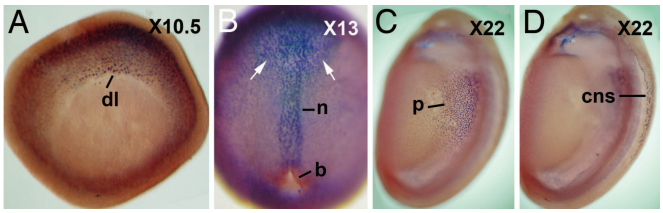

Fig. 3. The Lim1 immunostaining of *X. laevis* embryos. (*A*) Early gastrula. (*B*) Late gastrula. Lim1 is expressed in the notochord and in the anterior domain (arrows). (*C*) Neurula, focused on the pronephros anlage. (*D*) The same embryo shown in *C*, focused on the Lim1 expression in the CNS. b, blastopore; cns, central nervous system; dl, dorsal lip; n, notochord; p, pronephros.

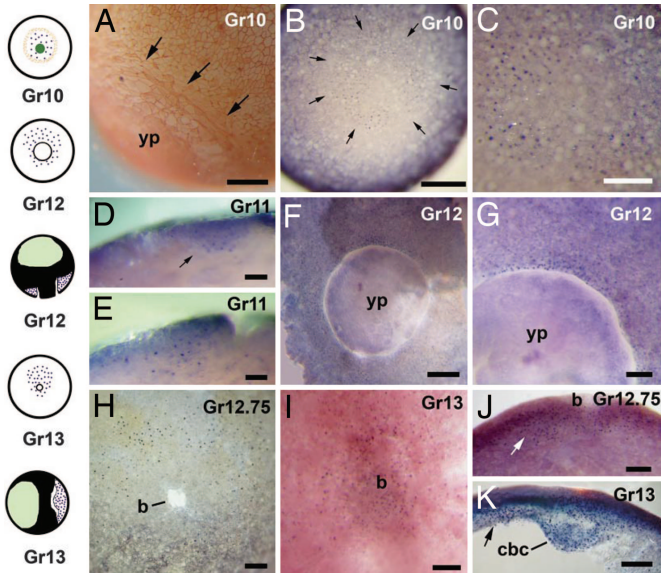

Fig. 4. Lim1 immunostaining in the *G. riobambae* gastrula. The vegetal pole is oriented toward the front in *B* and *C*, and the presumed dorsal side is oriented toward the top in *B*, *C*, and *F–I*. The dorsal side is oriented toward the left in *E*, *J*, and *K*. (*A*) The blastoporal rim (arrows) in an early gastrula that was stained for cell borders. (*B*) Lim1 expression (arrows) in an early gastrula. Higher numbers of Lim1-positive nuclei occur in the presumed dorsal side of this and later stages. (*C*) Higher magnification of the embryo shown in *B*. (*D*) Ventral region of a st-11 embryo in sagittal view. The Lim1 signal occurs in deep cells (arrow). (*E*) The dorsal lip of a st-11 embryo in sagittal view. (*F*) The ring of Lim1-positive nuclei around the blastopore of a midgastrula. (*G*) Higher magnification of the presumed dorsal side of the embryo shown in *F* (dorsal is toward the top). (*H*) The ring of Lim1-positive nuclei around the closing blastopore of a late gastrula. (*I*) Inner surface of the embryonic disk in an uncleared embryo. (*J*) Parasagittal section of an embryo at the time of blastopore closure. The Lim1 signal is more abundant in nuclei of the presumed dorsal side (arrow). (*K*) Sagittal section of the embryonic disk. The Lim1 signal is more abundant in nuclei of the dorsal side (arrow). The drawings on the left outline the *G. riobambae* Lim1 expression pattern: Lim1 signal is shown in purple, the blastoporal rim is shown in orange, the vegetal pole is shown in dark green, and the blastocoel is shown in light green. b, blastopore; cbc, circumblastoporal collar; dl, dorsal lip; yp, yolk plug; vp, vegetal pole. [Scale bars: 100 μm (*D* and *E*); 200 μm (*G* and *I–K*); 250 μm (*A*, *C*, and *H*); and 500 μm (*B* and *F*).]

The vegetal pole of *G. riobambae* st-10 embryos had three cell types that could be identified by a combination of morphological examination and expression of Lim1, the blastoporal rim, a deep ring of Lim1-positive cells that surrounded the vegetal pole, and the Lim1-negative cells located at the vegetal pole (Fig. 4 *A–C*). The blastoporal rim consisted of tiers of circumferentially elongated cells in the area of the future blastopore lip (Fig. 4*A*). In deep cells, a ring of Lim1-positive nuclei was found at the

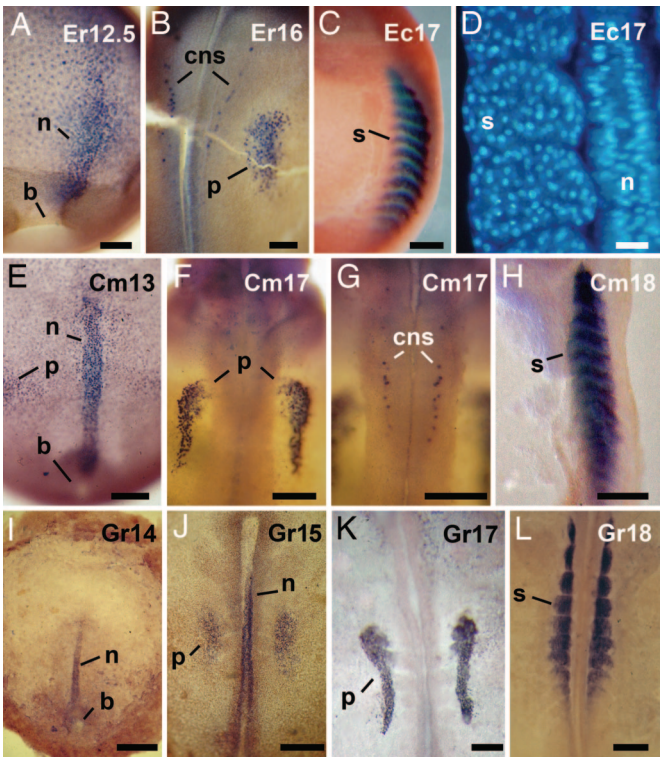

Fig. 5. Development of the notochord, pronephros, and cells of the CNS. Embryos of *E. randi* are shown in *A* and *B*, and embryos of of *E. coloradorum* are shown in *C* and *D*. (*A*) Expression of Lim1 in the notochord and anterior domain of a late gastrula. (*B*) Expression of Lim1 in the pronephros anlage and in cells of the CNS of a neurula. (*C*) Expression of myosin in the somites of a tailbud embryo. (*D*) Longitudinal section through the notochord and somites of a tailbud embryo, stained for cell nuclei. Embryos of *C. machalilla* are shown in *E–H*. (*E*) Expression of Lim1 in the notochord and precordal plate of a postgastrula. (*F*) Expression of Lim1 in the pronephros of a tailbud embryo. (*G*) Expression of Lim1 in cells of the CNS of the embryo shown in *F*. (*H*) Expression of myosin in the somites. Embryos of the marsupial frog *G. riobambae* are shown in *I–L*. (*I*) Expression of Lim1 in the notochord of a postgastrula. (*J*) Expression of Lim1 in the prospective pronephros of an early neurula. (*K*) Expression of Lim1 in the pronephros. (*L*) Expression of *cardiac actin* mRNA in the somites. b, blastopore; cns, central nervous system; n, notochord; p, pronephros; s, somite. [Scale bars: 50 μm (*D*); 100 μm (*A* and *B*); 200 μm (*F* and *G*); 250 μm (*C*, *E*, *H*, *K*, and *L*; and 500 μm (*I* and *J*).]

periphery of the future yolk plug (Fig. 4 *B* and *C*). It is unknown whether this Lim1-positive area overlapped with the blastoporal rim. The Lim1-positive ring was asymmetric, and a high number of Lim1-positive nuclei were detected toward one side, which may be the presumptive dorsal side. Inside this ring, the vegetal pole was Lim1-negative (Fig. 4 *B* and *C*). The vegetal pole undergoes vegetal contraction, and it is characterized by the presence of elongated cells of large size with small surface apices. The vegetal pole becomes incorporated into the yolk plug, as detected by the fate of vital stain marks (6, 7).

A ring of Lim1-positive nuclei continued to be present as the dorsal lip of the blastopore developed. Lim1-positive nuclei were more abundant in the dorsal lip of the blastopore than in the ventral side (Fig. 4 *D–F* and *H*). Few surface cells were Lim1-positive in the blastopore lip area (data not shown). Once the blastopore closed, deep cells of the embryonic disk were Lim1-positive (Fig. 4 *I* and *K*). In sections of the blastopore lip and embryonic disk, the Lim1-positive area was 10–12 cells wide (Fig. 4 *E* and *J*). In summary, a larger number of Lim1-positive nuclei were detected in the presumed dorsal side than in the ventral side of the gastrula from the onset of gastrulation in *G. riobambae* (Fig. 4 *B–K*).

Table 1. Modes of somitogenesis in frogs

Species	Egg size, mm	Gastrulation time, h*	Mode of somitogenesis	Refs.
X. laevis	1.3	14	cr	(28, 32)
E. randi	1.1	24	ci	
E. coloradorum	1.3	24	ci	
C. machalilla	1.6	96	ci	
E. anthonyi	2.0	96	ci	
E. tricolor	2.0	96	ci	
G. riobambae	3.0	336	ci	(33)
B. variegata	3.0	—	ci	(28)

cr, cell rotation; ci, cell interdigitation.
*Time from fertilization to the completion of gastrulation.

Notochord, Pronephros, Somites, and Neural Development. We compared formation of the notochord, the CNS, pronephros, and somites of *E. randi* and *E. coloradorum* (Fig. 5 *A–D*) with *C. machalilla* (Fig. 5 *E–H*) and *G. riobambae* (Fig. 5 *I–L*). The notochord in embryos of these frogs was Lim1-positive (Fig. 5 *A*, *E*, and *I*). The onset of notochord elongation, however, varied among species. The notochord was first detected in the midgastrula of *E. randi* (data not shown), and it was a prominent structure before closure of the blastopore (Fig. 5*A*), a pattern similar to that of *X. laevis*. In contrast, the notochord developed after blastopore closure in *C. machalilla* and *G. riobambae* (Fig. 5 *E* and *I*). The pronephros of the analyzed frogs was positive for Lim1 (Fig. 5 *B*, *F*, *J*, and *K*). Lim1 was also expressed in specific cells of the CNS in *E. randi* and *C. machalilla* (Fig. 5 *B* and *G*), whereas these cells were not identified in *G. riobambae* embryos (Fig. 5 *J* and *K*). It is unknown whether cells of the CNS are Lim1-positive at later stages of *G. riobambae* development. The patterns of Lim1 expression in *E. randi* (Fig. 5 *A* and *B*) and *E. coloradorum* embryos (data not shown) were similar.

We asked whether somite development was retarded in frogs with delayed elongation of the notochord. Somites were detected by expression of myosin in *E. coloradorum* and *C. machalilla* and by the expression of *cardiac actin* mRNA in *G. riobambae* and *X. laevis* embryos. The myosin expression patterns at the tailbud and later stages was strong in the embryos of the analyzed frogs (Fig. 5 *C* and *H*). The first detection of myosin expression, however, occurred earlier in the anterior somites of st-15 embryos of *E. coloradorum* and *E. randi* (data not shown). In contrast, in *C. machalilla*, the first myosin detection occurred later, in embryos of late st 17 (data not shown). The first expression of *cardiac actin* mRNA was observed in the anterior somites of st-15 embryos of *G. riobambae* (data not shown), and the signal became stronger at st 18 (Fig. 5*L*). In contrast, in *X. laevis* embryos, expression of *cardiac actin* mRNA was detected earlier, in the late gastrula (data not shown). Notochord and somite development in *E. coloradorum* and *E. randi* basically approached the developmental rate of *X. laevis* embryos, whereas the notochord and somite development was delayed in *C. machalilla* and *G. riobambae* embryos.

We investigated the mode of somitogenesis to further document the developmental pattern of the analyzed frogs (Table 1). In tailbud embryos (st 17) of *E. coloradorum* (Fig. 5*D*) and *E. randi* (data not shown), the somites consisted of numerous cells of round shape. At later stages, the myoblasts became elongated and interdigitated but did not span the length of the somite. Later, multinucleated myoblasts developed (data not shown). The mode of somitogenesis in embryos of three species of dendrobatid frogs (*C. machalilla*, *E. anthonyi*, and *E. tricolor*) was equivalent to the pattern observed in foam-nesting frogs (Fig. 5*D* and Table 1). This mode of somitogenesis is known as somitogenesis by cell interdigitation (28).

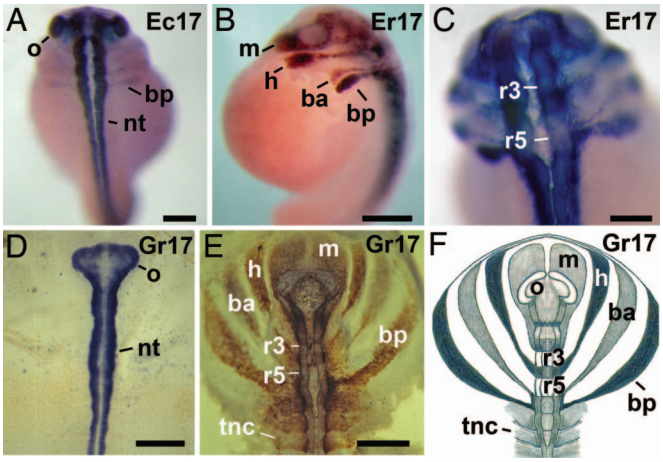

Fig. 6. Neural development. An embryo of *E. coloradorum* is shown in *A*, embryos of *E. randi* are shown in *B* and *C*, and embryos of *G. riobambae* are shown in *D–F*. (*A*) Dorsal view of a tailbud embryo immunostained against NCAM. The streams of CNC were faintly stained. (*B*) Lateral view of a tailbud embryo immunostained against antigen 2G9. (*C*) Dorsal view, in higher magnification, of the embryo in *B*. (*D*) Dorsal view of a st-17 embryo immunostained against NCAM. (*E*) Dorsal view of a st-17 embryo immunostained against antigen 2G9. The streams of cnc extend laterally in the flat embryo of *G. riobambae*. (*F*) Drawing of the antigen 2G9 expression in st-17 embryos of *G. riobambae*, modified from ref. 31. ba, branchial anterior stream of cnc cells; bp, branchial posterior stream of cnc cells; h, hyoid stream of cnc cells; m, mandibular stream of cnc cells; nt, neural tube; o, optic vesicle; r3, rhombomere 3; r5, rhombomere 5; tnc, trunk neural crest. [Scale bars: 200 μm (*C*); 250 μm (*A*); and 500 μm (*B*, *D*, and *E*).]

We studied the formation of the neural tube and the cranial neural crest (cnc) in embryos of the foam-nesting frogs in comparison with *G. riobambae*. Expression of the neural cell adhesion molecule (NCAM) was used to recognize the neural tube and of antigen 2G9 for detection of the neural crest (29–31). In all of the analyzed species, the first expression of NCAM and of antigen 2G9 occurred in st-14 embryos (data not shown), and the expression became stronger in tailbud embryos (Fig. 6). Antigen 2G9 is an uncharacterized and abundant neural protein, first detected in *X. laevis* (30). In embryos of *G. riobambae*, antigen 2G9 is expressed in the isthmus, rhombomeres 2 and 4, and rhombomeres caudal to rhombomere 5. It is also expressed in the streams of cnc and in the neural crest of the trunk as reported (31). The neural tube, the streams of cnc, and even numbered rhombomeres were clearly detected in tailbud embryos (st 17) of the foam-nesting frogs *E. randi* (Fig. 6 *A–C*) and *E. coloradorum* (data not shown). The patterns of NCAM and antigen 2G9 expression in embryos of foam-nesting frogs and *G. riobambae* were similar (Fig. 6 *D–F*).

Discussion

Development of *E. coloradorum* and *E. randi*. Egg size, developmental rate, and the mode of gastrulation of these frogs were comparable with *X. laevis*. Moreover, elongation of the notochord and, consequently, CE, started in the midgastrula in the embryos of foam-nesting frogs as in *X. laevis*. In contrast, tailbud embryos (st 17) differed not only morphologically (Fig. 1 *G* and *H*) but also in the pattern of somitogenesis (Table 1) and neural development (Figs. 5*D* and 6 *B* and *C*). Tailbud embryos of *E. coloradorum* and *E. randi* have a curved appearance (Fig. 1 *G* and *H*) and differ from the elongated tailbud of *X. laevis.* Moreover, the mode of somitogenesis and the size of cnc cell streams differed from *X. laevis*. Although cell rotation is the somitogenesis mode in *X. laevis* (28, 32), somitogenesis by cell interdigitation occurs in *Bombina variegata* and *G. riobambae*

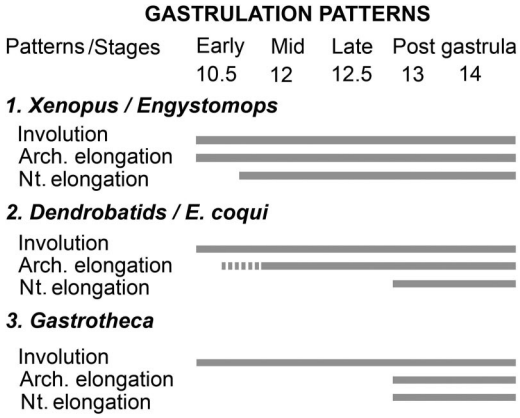

Fig. 7. Frog gastrulation patterns, modified from ref. 7. Three patterns of gastrulation were found according to developmental speed and overlap of processes. The broken bar indicates that the onset of archenteron elongation varies among frogs. The gastrulation patterns are explained in *Discussion*. arch, archenteron; n, notochord.

(28, 33) and in the foam-nesting and dendrobatid frogs analyzed in this work (Table 1). The mode of somitogenesis was not associated with egg size and developmental rate (Table 1). Other patterns of somitogenesis have been found in frogs and urodeles, as reviewed in ref. 34.

Development of the neural tube and the morphology of the streams of cnc cells are conserved features of frog development and resemble the basic pattern observed in *B. variegata* (31, 35). The cnc cell streams of *G. riobambae* and of foam-nesting frogs, however, are larger and more clearly defined than in *X. laevis*, *C. machalilla* (19, 31), and *E. tricolor* (data not shown). This analysis of development demonstrates that foam-nesting frogs are appropriate for developmental work.

Gastrulation Patterns. Three modes of gastrulation were previously defined that indicate that frog early development is composed of modules with differences in the relative timing of their occurrence (7). A similar conclusion was reached by the analysis of *X. laevis* embryos deficient in the expression of *dishevelled* (36). The present work extends the comparison of gastrulation patterns to frog species that differ in their reproductive strategies and time of development (Fig. 7). In *X. laevis*, *E. coloradorum*, and *E. randi*, whose small eggs develop rapidly, the processes of archenteron and notochord elongation overlap with involution (Fig. 7, pattern 1). In these frogs, CE starts in the midgastrula (Fig. 7, pattern 1). A different gastrulation trend was found among dendrobatid frogs and in the frog without tadpoles, *E. coqui* (Fig. 7, pattern 2), whose development is slower than in *X. laevis*. In these frogs, elongation of the archenteron and notochord is retarded. Notochord elongation and, consequently, CE begin in the post gastrula (7, 20, 26). Elongation of the archenteron, however, begins earlier in species with larger eggs, such as *E. coqui* (Fig. 2*J*), in comparison with embryos of the frog with smaller eggs, *C. machalilla* (7). Gastrulation in *G. riobambae* (Fig. 7, pattern 3) demonstrates that the major event of frog gastrulation is the involution of cells at the blastopore lip. Other aspects commonly associated with gastrulation, such as elongation of the archenteron and notochord and CE, occur after blastopore closure in the slow developing embryos of this frog (Fig. 7, pattern 3).

This study reveals that, in *E. coqui*, the archenteron elongates in the absence of CE (Fig. 2*J*), because archenteron elongation occurs during gastrulation, whereas the notochord elongates in the postgastrula (26). Archenteron elongation in *E. coqui* and other frogs that share its gastrulation pattern (Fig. 7, pattern 2)

resembles gastrulation in the sturgeon, where epiboly and elongation of the archenteron occur first, followed later by CE (37, 38). Several forces participate in the elongation of the archenteron, among them epiboly, CE, and vegetal rotation (36). Frog gastrulation patterns were unrelated to egg size, as seen by the gastrulation differences detected in the similarly large eggs of *G. riobambae* and *E. coqui* (Fig. 2 *B* and *J*). This study suggests that frog gastrulation patterns are related to the frog developmental strategies and possibly to their phylogeny rather than to the size of their eggs (Fig. 7).

Expression of Lim1 and the Dorsal Lip of *G. riobambae* Embryos. The dorsal side of the early *G. riobambae* gastrula was detected by the expression of the homeodomain protein Lim1 (Fig. 4). The dorsal lip of the blastopore of the *G. riobambae* gastrula is small and shallow. By the expression of Bra, the dorsal side of the *G. riobambae* gastrula was first detected after blastopore closure (4, 6, 7). As visualized by Lim1 expression, however, the dorsal side of *G. riobambae* embryos is detectable at the onset of gastrulation (Fig. 4 *B* and *C*).

The expression of Lim1 defines the dorsal lip of the blastopore, the notochord, cells of the CNS, and the pronephros in embryos of *G. riobambae*, foam-nesting, and dendrobatid frogs and allows comparison of developmental differences. Expression of Lim1 in the notochord indicates that CE started in the midgastrula of the foam-nesting frogs and *X. laevis* embryos (Figs. 3*B* and 5*A*). In contrast, in embryos of *G. riobambae* and *C. machalilla*, notochord elongation and CE were retarded until after closure of the blastopore (Fig. 5 *E* and *I*), as detected by Bra expression (4, 7, 20).

Although the pattern of Lim1 expression is conserved not only in frogs but also in other vertebrates (14, 16–18), the time of expression varies. In particular, there were expression variations in the gastrula of different frogs. For example in the early gastrula of *X. laevis* and *E. randi*, Lim1 is strongly expressed on the dorsal side, with some expression in the ventrolateral regions of the marginal zone. In contrast, in *G. riobambae*, Lim1 is expressed around the presumed marginal zone, forming a vegetally located ring of Lim1-positive cells. This pattern is comparable with the nearly homogenous ring of *lim1* expression of the zebrafish early gastrula (16). In the gastrula of *X. laevis* and *E. randi*, expression of Lim1 in the notochord and in an anterior domain, likely the prechordal plate, occurs simultaneously. In contrast, in the dendrobatid frog *C. machalilla*, the Lim1 expression in these two regions is separated in time. Lim1 expression in the anterior domain occurs during gastrulation, whereas expression of Lim1 in the notochord occurs after closure of the blastopore. Therefore, the pronounced expression of Lim1 in the dorsal lip of the blastopore of *X. laevis* embryos (Fig. 3*A*) probably relates to the overlap of several developmental processes and Lim1 expression domains (Fig. 7, pattern 1). The comparative analysis of Lim1 expression in various frogs indicates that, in the rapidly developing embryos of *X. laevis*, the dorsal lip of the blastopore is not a homogeneous field of gene expression. Moreover, the dorsal lip of the blastopore of the gastrula in other frogs may have molecular features that vary according to the speed of their early development.

Expression of *Xlim1* and *Xbra* Overlap in the Prospective Mesoderm of *X. laevis*. The gene *Xbra* is an early response gene to mesoderm induction and is expressed in a deep ring around the blastopore (39, 40). Similarly, a ring of *Xlim1*-positive cells was detected around the *X. laevis* blastopore (14, 41). The major difference is the unequal expression of *Xlim1* in the dorsal side, whereas *Xbra* was expressed in a uniform ring (14, 40). *Xlim1* expression identifies the prospective mesoderm in *X. laevis* embryos (13, 14). Similarly, the expression of Lim1 around the blastopore of different frogs may identify the prospective mesoderm. Accordingly, in *G. riobambae* embryos, mesoderm induction may be shifted vegetally in comparison with *X. laevis.* The observed differences are likely part of the different gastrulation strategies of these frogs. Cell lineage studies in *G. riobambae* and other frogs will aid in identification of the prospective mesoderm and the onset of CE movements.

Expression of Bra and Lim1 in the presumptive prospective mesoderm of *G. riobambae* and *C. machalilla* are separated in time, whereas the expression of *Xlim1* and *Xbra* coincide in the *X. laevis* early gastrula (41). In fact, a deep ring of Bra-positive cells was first detected in the late gastrula of these frogs, whereas, in *X. laevis*, the *Xbra*-positive ring is visible from the onset of gastrulation (4, 20, 39, 40). In contrast to Bra, the expression of Lim1 was detectable at the onset of gastrulation in *G. riobambae* (Fig. 4 *B* and *C*) and *C. machalilla* (data not shown). The observed natural dissociation in the expression of these genes suggests that their function is also dissociated in the gastrula of the analyzed frogs. Both *Xlim1* and *Bra* are important for gastrulation movements (15, 42, 43). It may be that *Bra* expression and its direct target, the planar cell polarity pathway and CE, are delayed in the mentioned frogs, because it is known that, in *X. laevis*, the planar cell polarity pathway and CE are downstream of *XBra* (43–45). In contrast, the movements of vegetal rotation, endomesoderm identity, convergence and thickening (12, 46), and involution at the blastopore lip occur earlier in these frogs and may be guided by the expression of Lim1. In support of this view, it is already known that embryos of *X. laevis* depleted of *Xlim1* fail in the involution of axial mesoderm, and the mesodermal cells fail in their separation from the ectoderm (15). In conclusion, the comparative analysis provides important tools to gain insights into gene function during frog early development.

Materials and Methods

Frogs, Embryos, and Staging. Embryos of *E. coloradorum* and *E. randi* were cultured within their foam nests that floated on the surface of a dish filled with water. The procedures for the maintenance of adults and the handling of embryos of *G. riobambae* and *C. machalilla* were described (19, 47).

The collection localities are as follows: adults of *C. machalilla* were collected from three localities, Rio Coaque, Pedernales, and Machalilla, Province of Manabí, Ecuador; *E. tricolor* was collected from Moraspungo, Cotopaxi, Ecuador; *G. riobambae* was purchased from Hyla, Quito, Ecuador, or was collected from Quisapincha, Province of Tungurahua, Ecuador. The authorization 016-IC-FAU-DNBAP-MA from the Ministry of the Environment, Ecuador, allowed the collection of frogs. Fixed embryos of *E. coqui* were donated by R. P. Elinson (Duquesne University, Pittsburgh, PA). Embryos of *E. ingeri*, *D. auratus*, and *E. randi* and adults of *E. coloradorum* were donated by L. A. Coloma and collaborators (Pontificia Universidad Católica del Ecuador).

The gastrulation stages of *G. riobambae* are according to ref. 7. Gastrulae of all frogs were staged according to the *X. laevis* normal table of stages until st 14 (3, 19). Thereafter, embryos were staged according to Gosner (25).

Embryo Fixation, Staining, and Sectioning. Embryo fixation and vibratome sectioning are described in ref. 7. The cell surface staining of embryos was according to ref. 48. To detect cell nuclei, some sections were stained with Hoechst 33258 (Sigma–Aldrich, St. Louis, MO), mounted in glycerol, and examined with fluorescent optics.

Antibody Preparation. Anti-Lim1 is a polyclonal Ab produced in rabbit against the C-terminal region (amino acids 275–403; Swissprot accession no. P29674) of the *X. laevis* homeodomain protein Lim1 fused to GST (GST-Lim1C). The Ab was affinity-

purified with a GST-Lim1C coupled to CNBr-activated Sepharose 4B column and used for whole-mount immunostaining.

Whole-Mount Immunostaining. Embryos were immunostained in whole mount with anti-Lim1 or with the following mAbs: anti-myosin (Ab MF-20), anti-NCAM (Ab 4d), or anti-antigen 2G9. The first two Abs were obtained from the Developmental Studies Hybridoma Bank (Iowa City, IA). The anti-antigen 2G9 was donated by E. A. Jones (University of Warwick, Warwick, U.K.) (30). The secondary Abs were sheep anti-rabbit IgG or sheep anti-mouse conjugated to alkaline phosphatase (Roche Molecular Biochemicals, Mannheim, Germany). Immunostaining was done as described (20, 49). Embryos were analyzed and photographed with a Stemi SV 6 and with an Axiophot (Zeiss, Oberkochen, Germany).

***In Situ* Hybridization.** The cross-species *in situ* hybridization of *G. riobambae* embryos with a *X. laevis cardiac actin* riboprobe was according to ref. 31. The probe is the same one used as described in refs. 50 and 51.

We thank E. Amaya (University of Manchester, Manchester, U.K.), E. A. Jones, and R. P. Elinson for the donation of a *cardiac actin* riboprobe, anti-antigen 2G9, and *E. coqui* fixed embryos, respectively; L. A. Coloma, S. Ron, and other members of the Herpetology laboratory at Pontificia Universidad Católica del Ecuador for the donation of embryos and adults of various frogs; A. Medina for neural immunostaining of *G. riobambae* embryos; O. D. Pérez for discussions and scientific help; L. E. López for obtaining the frogs; S. Tajima and I. Suetake (Osaka University, Osaka, Japan) for help in the purification of anti-Lim1; and I. B. Dawid for critical reading of the manuscript. This work was supported, in part, by a 2006 grant from the Pontificia Universidad Católica del Ecuador.

1. de Robertis EM (2006) *Nat Rev Mol Cell Biol* 7:296–302.
2. del Pino EM (1989) *Development (Cambridge, UK)* 107:169–187.
3. Nieuwkoop PD, Faber J (1994) *Normal Table of Xenopus laevis (Daudin)*, (Garland Publishing, New York).
4. del Pino EM (1996) *Dev Biol* 177:64–72.
5. del Pino EM, Elinson RP (1983) *Nature* 306:589–591.
6. Elinson RP, del Pino EM (1985) *J Embryol Exp Morphol* 90:223–232.
7. Moya I, Alarcón I, del Pino EM (2007) *Dev Biol* 304:467–478.
8. Ballard WW (1955) *J Exp Zool* 129:77–98.
9. Keller R (1978) *J Morphol* 157:223–248.
10. Hardin J, Keller R (1988) *Development (Cambridge UK)* 103:211–230.
11. Keller R (1986) in *Developmental Biology: A Comprehensive Synthesis*, ed Browder L (Plenum, New York), pp 241–327.
12. Keller R, Shook D (2004) in *Gastrulation from Cells to Embryo*, ed Stern CD (Cold Spring Harbor Lab Press, Cold Spring Harbor, NY).
13. Taira M, Jamrich M, Good PJ, Dawid IB (1992) *Genes Dev* 6:356–366.
14. Taira M, Otani H, Jamrich M, Dawid IB (1994) *Development (Cambridge, UK)* 120:1525–1536.
15. Hukriede NA, Tsang TE, Habas R, Khoo P-L, Steiner K, Weeks DL, Tam PPL, Dawid IB (2003) *Dev Cell* 4:83–94.
16. Toyama R, O'Connell ML, Wright CVE, Kuehn MR, Dawid IB (1995) *Development (Cambridge UK)* 121:383–391.
17. Karavanov AA, Saint-Jeannet JP, Karavanova I, Taira M, Dawid IB (1996) *Int J Dev Biol* 40:453–461.
18. Shawlot W, Behringer RR (1995) *Nature* 374:425–430.
19. del Pino EM, Ávila ME, Pérez OD, Benítez M-S, Alarcón I, Noboa V, Moya IM (2004) *Int J Dev Biol* 48:663–670.
20. Benítez M-S, del Pino EM (2002) *Dev Dyn* 225:592–596.
21. Davidson EH, Hough BR (1969) *J Exp Zool* 172:25–48.
22. Hough BR, Yancey PH, Davidson EH (1973) *J Exp Zool* 185:357–368.
23. del Pino EM, Elinson RP (2003) in *The Vertebrate Organizer*, ed Grunz H (Springer, Berlin), pp 359–374.
24. Townsend DS, Stewart MM (1985) *Copeia* 1985:423–436.
25. Gosner KL (1960) *Herpetologica* 16:183–190.
26. Ninomiya H, Zhang Q, Elinson RP (2001) *Dev Biol* 236:109–123.
27. Kodjabachian L, Karavanov AA, Hikasa H, Hukriede NA, Aoki T, Taira M, Dawid IB (2001) *Int J Dev Biol* 45:209–218.
28. Kielbowna L (1981) *J Embryol Exp Morphol* 64:295–304.
29. Watanabe M, Freilinger AL, Rutishauser U (1986) *J Cell Biol* 103:1721–1727.
30. Jones EA, Woodland HR (1989) *Development (Cambridge, UK)* 107:785–791.
31. del Pino EM, Medina A (1998) *Int J Dev Biol* 42:723–731.
32. Hamilton L (1969) *J Embryol Exp Morphol* 22:253–264.
33. Gatherer D, del Pino EM (1992) *Int J Dev Biol* 36:283–291.
34. Radice GP, Neff AW, Shim YH, Brustis J-J, Malacinski GM (1989) *Int J Dev Biol* 33:325–343.
35. Olsson L, Hanken J (1996) *J Morphol* 229:105–120.
36. Ewald AJ, Peyrot SM, Tyszka JM, Fraser SE, Wallingford JB (2004) *Development (Cambridge, UK)* 131:6195–6209.
37. Bolker JA (1993) *J Exp Zool* 266:116–131.
38. Bolker JA (1993) *J Exp Zool* 266:132–145.
39. Smith JC, Price BMJ, Green JBA, Weigel D, Herrmann BG (1991) *Cell* 67:79–87.
40. Gont LK, Steinbeisser H, Blumberg B, De Robertis EM (1993) *Development (Cambridge, UK)* 119:991–1104.
41. Taira M, Saint-Jeannet JP, Dawid IB (1997) *Proc Natl Acad Sci USA* 94:895–900.
42. Herrmann BG, Kispert A (1994) *Trends Genet* 10:280–286.
43. Smith J (1999) *Trends Genet* 15:154–158.
44. Conlon FL, Smith JC (1999) *Dev Biol* 213:85–100.
45. Tada M, Smith JC (2000) *Development (Cambridge, UK)* 127:2227–2238.
46. Keller R, Danilchik M (1988) *Development (Cambridge, UK)* 103:193–209.
47. Elinson RP, del Pino EM, Townsend DS, Cuesta FC, Eichhorn P (1990) *Biol Bull* 179:163–177.
48. Kageyama T (1980) *Dev Growth Differ* 22:659–668.
49. Kuratani S, Horigome N (2000) *Zool Sci* 17:893–909.
50. Hemmati-Brivanlou A, Frank D, Bolce ME, Brown BD, Sive HL, Harland RM (1990) *Development (Cambridge, UK)* 110:325–330.
51. Amaya E, Musci TJ, Kirschner MW (1991) *Cell* 66:257–270.